



OPEN ACCESS

EDITED BY

Maria Carolina Touz,
Medical Research Institute Mercedes and
Martin Ferreyra (INIMEC), Argentina

REVIEWED BY

Yong Fu,
Washington University in St. Louis,
United States
Veronica Risco-Castillo,
INRA École Nationale Vétérinaire d'Alfort
(ENVA), France

*CORRESPONDENCE

Camilo Larrazabal
✉ Clarrazabal@uct.ac.za
Liliana M. R. Silva
✉ liliana.silva@vetmed.uni-giessen.de

RECEIVED 25 June 2024

ACCEPTED 26 July 2024

PUBLISHED 09 August 2024

CITATION

Larrazabal C, Hermosilla C, Taubert A and
Silva LMR (2024) *Besnoitia besnoiti* tachyzoite
replication in bovine primary endothelial cells
relies on host Niemann–Pick type C protein 1
for cholesterol acquisition.
Front. Vet. Sci. 11:1454855.
doi: 10.3389/fvets.2024.1454855

COPYRIGHT

© 2024 Larrazabal, Hermosilla, Taubert and
Silva. This is an open-access article
distributed under the terms of the [Creative
Commons Attribution License \(CC BY\)](https://creativecommons.org/licenses/by/4.0/). The
use, distribution or reproduction in other
forums is permitted, provided the original
author(s) and the copyright owner(s) are
credited and that the original publication in
this journal is cited, in accordance with
accepted academic practice. No use,
distribution or reproduction is permitted
which does not comply with these terms.

Besnoitia besnoiti tachyzoite replication in bovine primary endothelial cells relies on host Niemann–Pick type C protein 1 for cholesterol acquisition

Camilo Larrazabal^{1,2*}, Carlos Hermosilla¹, Anja Taubert¹ and Liliana M. R. Silva^{1,3,4*}

¹Institute of Parasitology, Biomedical Research Center Seltersberg, Justus Liebig University Giessen, Giessen, Germany, ²Department of Veterinary Sciences and Public Health, Universidad Católica de Temuco, Temuco, Chile, ³Egas Moniz Center for Interdisciplinary Research (CiiEM), Egas Moniz School of Health & Science, Caparica, Almada, Portugal, ⁴MED-Mediterranean Institute for Agriculture, Environment and Development & CHANGE-Global Change and Sustainability Institute, Universidade de Évora, Évora, Portugal

Besnoitia besnoiti is a cyst-forming apicomplexan parasite and the causal agent of bovine besnoitiosis. During early phase of infection, tachyzoites replicate within host endothelial cells in a host cell cholesterol-dependent process. By applying U18666A treatments, we here evaluated the role of Niemann–Pick type C protein 1 (NPC1) in both, intracellular *B. besnoiti* replication and host cellular cholesterol distribution. Additionally, *B. besnoiti*-driven changes in NPC1 gene transcription were studied by qPCR. Overall, U18666A treatments significantly reduced *B. besnoiti* proliferation and induced cholesterol accumulation in host cytoplasmic dense vesicles. However, NPC1 gene transcription was not affected by *B. besnoiti* infection.

KEYWORDS

Besnoitia besnoiti, Niemann–Pick type C protein, NPC1, U18666A, cholesterol

Introduction

Besnoitia besnoiti is an obligate intracellular apicomplexan parasite belonging to the cyst-forming group of coccidia, and represents the causative agent of bovine besnoitiosis, a cattle disease reemerging in Europe (1). In this context, clinical bovine besnoitiosis is provoked by tachyzoite proliferation and characterized by general symptoms, such as fever, lethargy, tachycardia, tachypnea, congested mucosae, edema, anorexia, and weight loss during acute infection phase, while the chronic phase is marked by bradyzoites cyst formation causing significant skin alterations and potential bull infertility (1, 2). Overall, during the febrile acute stage of besnoitiosis, tachyzoites primarily proliferate within endothelial cells of various organs and vessels, leading to vasculitis, thrombosis, and necrosis of venules and arterioles (1, 3, 4). In line, cumulated *in vitro* evidence has confirmed the suitability of primary bovine endothelial cell lines for *B. besnoiti* infection and proliferation, with replication rates similar to other coccidian parasites, such as *Toxoplasma gondii* or *Neospora caninum*, resulting in host cell lysis after 48 to 72 h (5–8), thereby effectively serving as an *in vitro* host cell model that closely mimics the *in vivo* scenario.

Like other coccidian parasites, intracellular replication of *B. besnoiti* is characterized by a rapid proliferation of tachyzoites (7, 8), therefore requiring a huge amount of cell building blocks. However, apicomplexans have undergone gene losses and consequently lack molecules essential for cholesterol biosynthesis (9). Therefore, to fulfil their molecular requirements, apicomplexan parasites employ diverse strategies, such as host organelle sequestration, host cell molecule scavenging and host gene modulation (10–12). Physiologically, cellular cholesterol can be acquired by both *de novo* biosynthesis and uptake from extracellular sources, with the latter significantly relying on low density lipoprotein (LDL)-based cholesterol endocytosis (13, 14). Mechanistically, plasmatic LDL particles are bound to LDL receptors (LDLR), and LDL-LDLR complexes are formed in a clathrin-dependent process, being internalized later (13, 14). This endocytic product undergoes hydrolysis within early endosomes being enriched with acid-containing vesicles, finally allowing LDLR recycling to the cytoplasmic membrane. Simultaneously, LDL-derived cholesterol is cleaved by acid lipase activity and thereafter incorporated as free cholesterol into the endoplasmic reticulum (ER) (13, 14). Notably, the hydrophobic nature of cholesterol requires its transport from late endosomes to the ER, a process facilitated by sterol carrier proteins (13, 14). In mammals, this transport is largely dependent on the Niemann–Pick type C protein 1 (NPC1). Cholesterol then is esterified and stored as cholesteryl esters together with other neutral lipids in cytoplasmic lipid droplets, which have been demonstrated to be scavenged by apicomplexan parasites (10, 11, 15, 16). In this context, the pivotal role of host NPC1 in cholesterol acquisition has been reported for other apicomplexans, such as *T. gondii*, *N. caninum*, *Plasmodium* spp., and *Eimeria bovis* (10, 11, 17, 18). Intriguingly, studies on *B. besnoiti* tachyzoite proliferation have revealed a dual participation of both LDL-driven and *de novo* biosynthesis-based cholesterol pathways (8), suggesting that *B. besnoiti* may differ from other fast proliferating apicomplexans in terms of cholesterol acquisition. Hence, the primary objective of this study was to assess the role of NPC1 in *B. besnoiti* replication in primary endothelial cells.

Methods

Primary host cell and *Besnoitia besnoiti* tachyzoites culture

Primary bovine umbilical vein endothelial cells (BUVEC) were used in this study given its suitability for infection and proliferation, and the *in vivo* endothelial tropism of *B. besnoiti* tachyzoites (4, 8). BUVEC were isolated according to established methods (19). Cells were maintained at 37°C in a 5% CO₂ atmosphere in a modified endothelial cell growth medium (modECGM), composed by ECGM medium (PromoCell) diluted in 1:3 ratio with M199 (Sigma-Aldrich) and supplemented with 500 U/mL penicillin (Sigma-Aldrich), 50 µg/mL streptomycin (Sigma-Aldrich) and 5% fetal calf serum (FCS; Biochrom). As a primary cell type, only BUVEC isolates at less than three passages were utilized.

B. besnoiti tachyzoite stages (strain *Bb Evora04*) were propagated by successive passages in Madin Darby bovine kidney cells (MDBK) as described elsewhere (8). Cells were cultured in RPMI medium (Sigma-Aldrich), supplemented and maintained as described above. Vital parasites were harvested from infected host cell supernatants, pelleted (800 × g; 5 min) and re-suspended in modECGM for immediate further experiments.

Inhibitor treatment

Pharmacological inhibition of NPC1 was achieved by the NPC1 blocker U18666A (20) (Cayman, diluted in DMSO; 23 mM). U18666A was diluted in modECGM at varying concentrations (0.93–7.5 µM), with confirmed non-cytotoxic effect on BUVEC as described elsewhere (18). Treatments were applied to fully confluent cell monolayers seeded on fibronectin-coated 12-well plates (Sarstedt; 1:400; Sigma-Aldrich) 48 h prior to infection. At this point, the inhibitor was removed, cells were washed to remove any traces of U18666A and were infected with *B. besnoiti* tachyzoites at a multiplicity of infection (MOI) of 1:5. The infection process lasted for 4 h under inhibitor-free conditions. Then, extracellular tachyzoites were removed and the inhibitor was added again to the cell culture medium. At 48 h *post infectionem* (p. i.), tachyzoites present in cell culture supernatants were collected, pelleted (800 × g; 5 min) and quantified using a Neubauer chamber. Diluted DMSO was included as vehicle control setting.

Live cell 3D-holotomographic microscopy

To visualize the effects of U18666A treatments on parasite development and host cellular cholesterol distribution, BUVEC were seeded on 35 mm tissue culture µ-dishes (Ibidi®), treated with U18666A (7.5 µM) or vehicle (DMSO) and infected with *B. besnoiti* tachyzoites (MOI of 3:1). At 24 h p. i., 3D-holotomographic microscopy was performed using a 3D Cell-Explorer (Nanolive). Microscopic data were analyzed by STEVE software (Nanolive) to generate refractive index (RI)-based z-stacks. Thereafter, the average pixel intensity was estimated in the area surrounding each cell (defined as region of interest) from max-intensity projected RI maps by ImageJ software v1.54 (21), based on the correlation between RI and cell-dry matter content (22).

Cholesterol visualization and quantification

Cellular free cholesterol distribution was visualized via filipin III staining [35 µg/mL; 1 h, 37°C; Cayman (23),] in *B. besnoiti*-infected cells and non-infected controls (seeded on 35 mm tissue culture µ-dishes, Ibidi), via epifluorescence using the 3D Cell-Explorer (Nanolive). Additionally, to determine the impact of U18666A on BUVEC neutral lipid content, cells were seeded into 25 cm² flasks (Sarstedt) and treated with U18666A (7.5 µM) for 48 h. Thereafter, cells were collected, pelleted and stained with BODIPY 493/503 (2 µg/mL; 1 h, 37°C, Cayman) as described elsewhere (8, 18), and analyzed by flow cytometry (Accuri C6®, Becton-Dickinson). Finally, cells were gated according to their size and granularity; BODIPY 493/503-derived signals were assessed in the FL-1 channel as previously described (12, 17).

RT-qPCR for relative quantification of NPC1 mRNA

To evaluate the effects of *B. besnoiti* infection on host cellular NPC1 gene transcription, qPCR of *B. besnoiti*-infected cell was performed. BUVEC were cultivated in 25 cm² tissue culture flasks (Greiner) and infected with *B. besnoiti* tachyzoites (MOI = 5:1). At 3, 6, 12 and 24 h p. i., infected host cells and non-infected controls were processed for RNA

isolation by RNeasy kit (Qiagen), according to manufacturer's instructions. Contaminating genomic DNA was removed by DNA digestion (10U DNase I, Thermo Scientific) following manufacturer's instructions. The efficacy of genomic DNA digestion was confirmed by no-RT-controls in each RT-qPCR experiment. For cDNA synthesis, SuperScript IV (Invitrogen) was used in accordance with manufacturer's instructions. The probes, labeled at the 5'-end with a reporter dye FAM (6-carboxyfluorescein) and at the 3'-end with the quencher dye TAMRA (6-carboxytetramethyl-rhodamine), were designed for NPC1 with the following sequences: *Bos taurus* NPC1 forward 5'-TCTGGAGATAAGAGATACAAC-3'; reverse 5'-CTGACATTGCCAAAGAAG-3', and probe CACCAGAGCCATTGCCACAG. qPCR-based DNA amplification was conducted on a Rotor-Gene Q Thermocycler (Qiagen) in duplicates within a 10 μ L total volume containing 400 nM forward and reverse primers, 200 nM probe, 10 ng cDNA, and 5 μ L 2 \times PerfeCTa qPCR FastMix (Quanta Biosciences). The reaction conditions included an initial step at 95°C for 5 min, followed by 45 cycles at 94°C for 15 s, 60°C for 60 s, and 72°C for 30 s. Relative gene transcription quantification was performed using $\Delta\Delta$ Ct method where GAPDH served as the reference housekeeping gene, as reported previously (8).

Statistical analysis

Statistical analyses were carried out with the software GraphPad® Prism 8 (version 8.4.3.). Data description included arithmetic mean \pm standard deviation of five biological replicates. In addition, the non-parametric statistical Mann–Whitney test for comparison of two experimental conditions was applied. In cases of three or more conditions, Kruskal–Wallis test was used. Whenever global comparison by Kruskal–Wallis test indicated significance, *post hoc* multiple comparison tests were carried out by Dunn tests to compare test with control conditions. Outcomes of statistical tests were considered to indicate significant differences when $p \leq 0.05$ (significance level).

Results

U18666A treatment inhibits *Besnoitia besnoiti* tachyzoite proliferation and induces dense vesicle accumulation

The participation of host NPC1 on *B. besnoiti* proliferation was determined by treatments with its specific inhibitor U18666A. Overall, pharmacological blockage of NPC1 by 7.5 μ M U18666A treatments led to a significant reduction ($p=0.003$) of *B. besnoiti* replication by $56.4 \pm 12.96\%$ (IC_{50} : $10.42 \mu\text{M} \pm 2.36$; Figure 1A) at 48 h p. i. Likewise, live cell 3D holotomography of *B. besnoiti* meront development in U18666A-treated host cells showed less parasitophorous vacuoles (PV) each containing fewer tachyzoites, visibly affected in morphology at 24 h p. i., when compared with vehicle-treated host cells (Figure 1B). Additionally, U18666A treatments (7.5 μ M) led to an accumulation of refractive-dense vesicles (average RI 1.358 ± 0.005 ; $n=100$ vesicles) within the cytoplasm of infected and non-infected BUVEC (Figure 2A). In line, single cell analysis revealed an increase in RI average by 13.01% ($p < 0.0001$) driven by U18666A treatments (Figure 2B). Finally, no effect on *B. besnoiti* tachyzoite infectivity was observed after a 30 min treatment of free tachyzoites with U18666A at 7.5 μ M (Supplementary Figure S1).

U18666A treatment affects cholesterol distribution, without inducing neutral lipids accumulation

Given the effect observed by U18666A treatments on RI-based maps, its effect on cellular total cholesterol distribution and neutral lipid content was evaluated by filipin III and BODIPY 493/503 staining, respectively (22). Overall, an inhibitor (U18666A)-driven translocation of filipin III-derived cholesterol signals from cytoplasmic membranes into cytoplasmic vesicles was detected (Figure 2C). In contrast and reflecting cellular neutral lipid content, no statistical significant ($p=0.095$) effect of U18666A treatments on BODIPY 493/503-derived total signal intensities was observed (Figure 2D) indicating an U18666A-mediated effect on subcellular cholesterol/neutral lipid distribution, but not on its total amount.

The NPC1 gene is not modulated by *Besnoitia besnoiti* infection in BUVEC

Since apicomplexan parasites are capable of modulating host gene expression to ensure their obligate intracellular replication metabolic requirements, the effect of *B. besnoiti* infection on NPC1 mRNA expression in BUVEC was evaluated over time by RT-qPCR. Even though NPC1 gene transcription revealed slightly enhanced at 12 and 24 h p. i. in single endothelial cell isolates (Figure 3), no significant *B. besnoiti* infection-driven changes in NPC1 gene expression were stated.

Discussion

Considering that apicomplexan parasites are auxotrophic for cholesterol, they rely on host cellular sterol sources to satisfy their molecular requirements for obligate intracellular proliferation (9). In this context, LDL-based cholesterol uptake represents a typical cholesterol source for obligate intracellular apicomplexan species. Overall, based on the key role of LDL endocytic routes, here we explored the participation of NPC1 in *B. besnoiti* tachyzoite proliferation, thereby presenting the first report on this sterol carrier for *B. besnoiti* infections in primary bovine endothelial cells. In detail, a pivotal role of NPC1 for *B. besnoiti* replication was confirmed since pharmacological NPC1 blockage by U18666A (7.5 μ M) treatments significantly inhibited tachyzoite replication in BUVEC, with an overall reduction of 56.4%. In line, former reports already indicated a principle antimicrobial capacity of NPC1 blockage for different virus infections like hepatitis C virus, Ebola virus, Dengue virus, Pseudorabies virus, and feline coronavirus (24–27). Referring to apicomplexan parasites, NPC1-related data are relatively scarce. Nonetheless, prior work showed that U18666A treatments (2.3 μ M) reduced *T. gondii* replication by 72% in CHO cells (10). Likewise, NPC1 blockage also interfered with *E. bovis* macromeront development in BUVEC (18). Moreover, U18666A treatments not only impaired *Plasmodium berghei* schizont development in Heh7 cells, MEF cells and primary hepatocytes, but also reduced parasite burden in mice *in vivo* (17), suggesting a general, NPC1-related mechanism in apicomplexan intracellular replication. Interestingly, current findings demonstrated only a partial effect of NPC1 inhibition on *B. besnoiti* development thereby implying alternative routes of cholesterol acquisition.

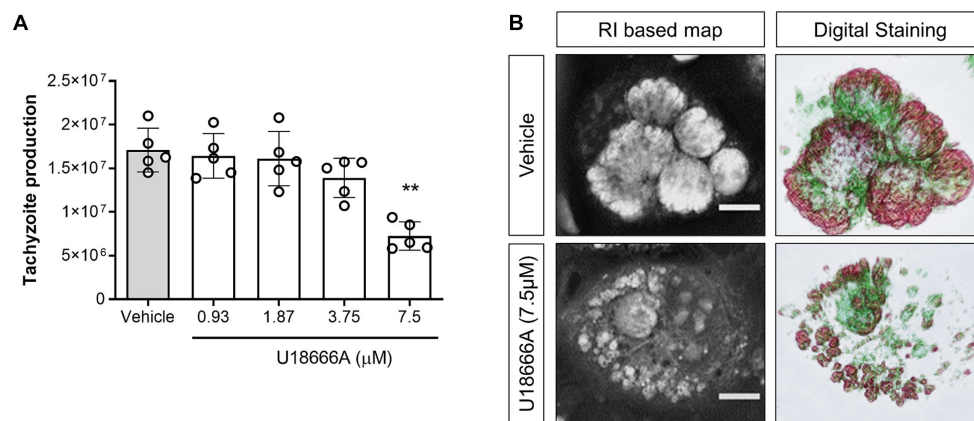


FIGURE 1

NPC1 inhibition reduces *B. besnoiti* intracellular proliferation. **(A)** BUVEC were treated with U18666A (0.93, 1.87, 3.75 and 7.5 μM) 48 h before *B. besnoiti* infection (MOI 1:5). At 48 h p. i., the number of tachyzoites present in cell culture supernatants were counted. **(B)** Exemplary illustration of live cell 3D holotomography and digital staining of vehicle- or U18666A (7.5 μM)-treated *B. besnoiti*-infected BUVEC at 24 h p. i. Scale bar represents 5 μm . Bars represent means of five biological replicates \pm standard deviation. ** $p \leq 0.01$.

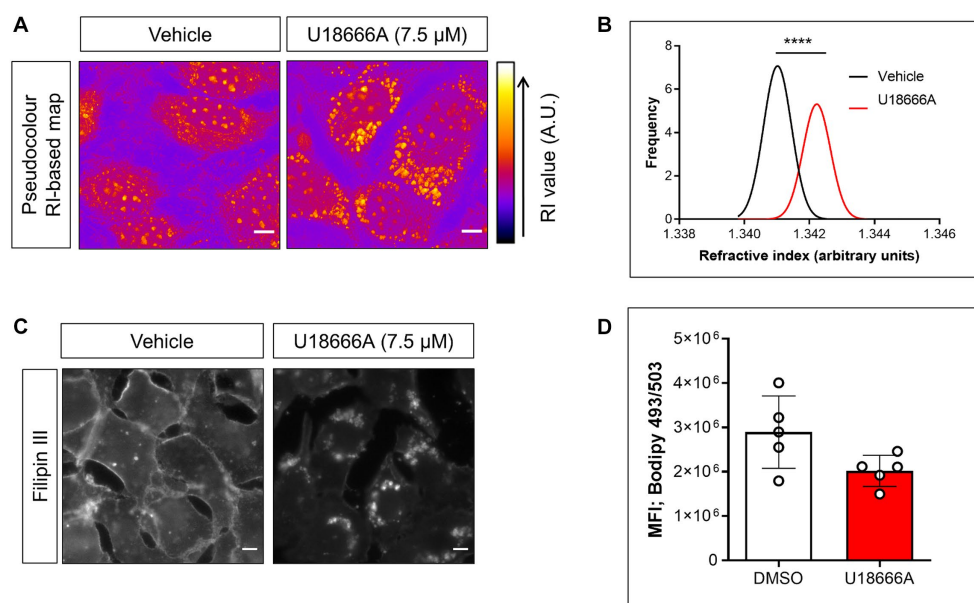
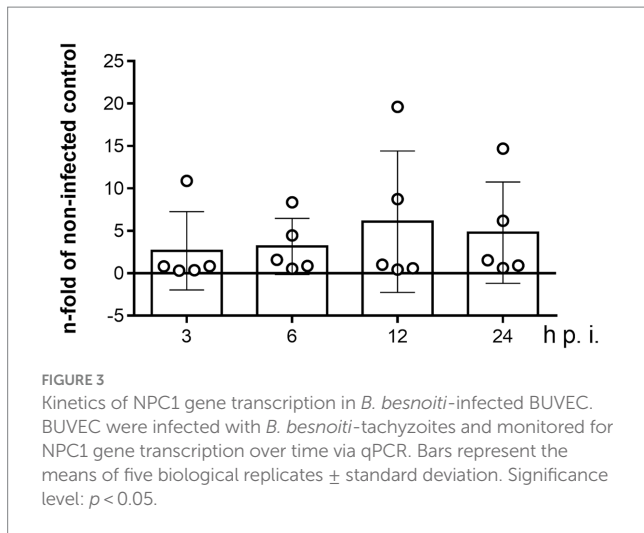


FIGURE 2

U18666A treatment affects subcellular cholesterol distribution and single cell RI without changing cellular neutral lipid content. **(A)** Live cell holotomography-deduced RI based images of vehicle- or U18666A (7.5 μM)-treated BUVEC depicted in pseudocolour. **(B)** Frequency histogram of single cell-based average RI of vehicle- or U18666A (7.5 μM)-treated cells. **(C)** Filipin III-driven fluorescence signals of vehicle- or U18666A (7.5 μM)-treated BUVEC. **(D)** Flow cytometry-based quantification of BODIPY 493/503-derived fluorescence signals of vehicle- or U18666A (7.5 μM)-treated cells. Scale bar represents 5 μm . Bars represent means of five biological replicates \pm standard deviation. **** $p \leq 0.0001$.

In agreement, coccidia-driven upregulation of *de novo* cholesterol biosynthesis and cholesterol uptake from extracellular sources by other receptors like OLR-1 or SR-BI have been proposed (6, 8). Mechanistically, U18666A treatments prevent the exit of cleaved cholesteryl esters from late endosomes, thus driving free cholesterol accumulation in these organelles (20). In this context, we first assessed NPC1 blockage in U18666A-treated BUVEC by 3D live cell holotomography, permitting a functional insight into live cell morphology through refractive properties assessment (28). Here, a significant accumulation of refractive-dense vesicles in the cytoplasm of U18666A-treated BUVEC was detected. The morphological

characteristics of these vesicles matched with a prior report on U18666A-treated HeLa cells where these structures were identified as late endosomes (28). Moreover, the impact of NPC1 blockage on cholesterol transport in primary bovine endothelial cells was confirmed by filipin III-based staining of cholesterol. Hence, U18666A treatments caused a subcellular redistribution of filipin III-based signals from evenly stained membranes in non-treated cells into visible cytoplasmic vesicles in treated BUVEC. Physiologically, intracellular cholesterol levels are tightly regulated by feedback mechanisms that operate at transcriptional levels. The content of cholesterol/cholesteryl esters triggers the upregulation of molecules that mediate their efflux (i.e.,



ABCA1) (29). In line, FACS-based analyses showed no changes in total BODIPY 493/503-derived signals in U18666A-treated BUVEC, indicating that NPC1 blockage does not induce changes in total cholesterol/cholesteryl ester content but exclusively drives subcellular compartmentalization of these sterols which then are unavailable for cytoplasmic *B. besnoiti* stages consumption within PV.

Host cell gene modulation is a mechanism widely reported to support the successful replication of other apicomplexan parasites (30, 31). Nonetheless, NPC1 regulation in apicomplexan-parasitized host cells is not fully understood. However, it is linked to a sterol-regulatory binding protein (SRBP)-dependent mechanism, with lipid availability and downstream cholesterol metabolite abundance regulating NPC1 gene expression (32, 33). Despite that, NPC1 overexpression increased sterol esterification in CHO cells (34). Therefore, we also analysed the capacity of *B. besnoiti* tachyzoites to modulate NPC1 gene expression over time. Unexpectedly, no infection-driven changes on NPC1 on the transcriptional level were noted. This contrasts with findings on the closely related parasite *N. caninum*, in which transcriptomic analysis of infected trophoblastic cells revealed an upregulation of this gene at 8 h p. i (30, 35).

In conclusion, the current findings confirm a participation of NPC1 in *B. besnoiti* merogonic proliferation in BUVEC, thereby highlighting the role of this host protein in apicomplexan biology. Further analyses are needed to evaluate whether the blockage of cholesterol redistribution via NPC1 inhibition may represent a potential therapeutic target not only against cyst-forming-but also against non-cyst-forming-coccidian parasites.

Data availability statement

The raw data supporting the conclusions of this article will be made available by the authors, without undue reservation.

Ethics statement

Ethical approval was not required for the studies on animals in accordance with the local legislation and institutional requirements because only commercially available established cell lines were used.

Author contributions

CL: Conceptualization, Formal analysis, Investigation, Writing – original draft, Writing – review & editing. CH: Project administration, Resources, Visualization, Writing – review & editing. AT: Conceptualization Funding acquisition, Resources, Supervision, Writing – review & editing. LS: Conceptualization Formal analysis, Investigation, Supervision, Writing – review & editing, Writing – original draft.

Funding

The author(s) declare that no financial support was received for the research, authorship, and/or publication of this article.

Acknowledgments

The authors would like to thank Christine Henrich, Dr. Christin Ritter, and Hannah Salecker for their outstanding technical support. The authors also are very thankful to Prof. Dr. A. Wehrend (Clinic for Obstetrics, Gynaecology and Andrology of Large and Small Animals, Justus Liebig University, Giessen, Germany) for the continuous supply of bovine umbilical cords.

Conflict of interest

The authors declare that the research was conducted in the absence of any commercial or financial relationships that could be construed as a potential conflict of interest.

The author(s) declared that they were an editorial board member of Frontiers, at the time of submission. This had no impact on the peer review process and the final decision.

Publisher's note

All claims expressed in this article are solely those of the authors and do not necessarily represent those of their affiliated organizations, or those of the publisher, the editors and the reviewers. Any product that may be evaluated in this article, or claim that may be made by its manufacturer, is not guaranteed or endorsed by the publisher.

Supplementary material

The Supplementary material for this article can be found online at: <https://www.frontiersin.org/articles/10.3389/fvets.2024.1454855/full#supplementary-material>

SUPPLEMENTARY FIGURE S1
U18666A does not affect *B. besnoiti* infectivity in BUVEC. *B. besnoiti* tachyzoites were exposed to either the vehicle or U18666A for 30 min and then allowed to infect BUVEC monolayers. Bars represent the means of five biological replicates \pm standard deviation.

References

- Alvarez-García G, Frey CF, Mora LMO, Schares G. A century of bovine besnoitiosis: an unknown disease re-emerging in Europe. *Trends Parasitol.* (2013) 29:407–15. doi: 10.1016/j.pt.2013.06.002
- Cortes H, Leitão A, Gottstein B, Hemphill A. A review on bovine besnoitiosis: a disease with economic impact in herd health management, caused by *Besnoitia besnoiti* (Franco and Borges, 1916). *Parasitology.* (2014) 141:1406–17. doi: 10.1017/S0031182014000262
- Álvarez-García G, García-Lunar P, Gutiérrez-Expósito D, Shkap V, Ortega-Mora LM. Dynamics of *Besnoitia besnoiti* infection in cattle. *Parasitology.* (2014) 141:1419–35. doi: 10.1017/S0031182014000729
- Langenmayer MC, Gollnick NS, Majzoub-Altweck M, Scharr JC, Schares G, Hermanns W. Naturally acquired bovine besnoitiosis: histological and immunohistochemical findings in acute, subacute, and chronic disease. *Vet Pathol.* (2015) 52:476–88. doi: 10.1177/0300985814541705
- Larrazabal C, Silva LMR, Hermosilla C, Taubert A. Ezetimibe blocks *Toxoplasma gondii*-, *Neospora caninum*- and *Besnoitia besnoiti*-tachyzoite infectivity and replication in primary bovine endothelial host cells. *Parasitology.* (2021) 148:1107–15. doi: 10.1017/S0031182021000822
- Larrazabal C, López-Osorio S, Velásquez ZD, Hermosilla C, Taubert A, Silva LMR. Thiosemicarbazone copper chelator BLT-1 blocks apicomplexan parasite replication by selective inhibition of scavenger receptor B type 1 (SR-BI). *Microorganisms.* (2021) 9:2372. doi: 10.3390/microorganisms9112372
- Jiménez-Meléndez A, Fernández-Álvarez M, Calle A, Ramírez MÁ, Diezma-Díaz C, Vázquez-Arbaizar P, et al. Lytic cycle of *Besnoitia besnoiti* tachyzoites displays similar features in primary bovine endothelial cells and fibroblasts. *Parasit Vectors.* (2019) 12:517. doi: 10.1186/s13071-019-3777-0
- Silva LMR, Lütjohann D, Hamid P, Velásquez ZD, Kerner K, Larrazabal C, et al. *Besnoitia besnoiti* infection alters both endogenous cholesterol *de novo* synthesis and exogenous LDL uptake in host endothelial cells. *Sci Rep.* (2019) 9:6650. doi: 10.1038/s41598-019-43153-2
- Coppens I. Targeting lipid biosynthesis and salvage in apicomplexan parasites for improved chemotherapies. *Nat Rev Microbiol.* (2013) 11:823–35. doi: 10.1038/nrmicro3139
- Coppens I, Sinai AP, Joiner KA. *Toxoplasma gondii* exploits host low-density lipoprotein receptor-mediated endocytosis for cholesterol acquisition. *J Cell Biol.* (2000) 149:167–80. doi: 10.1083/jcb.149.1.167
- Nolan SJ, Romano JD, Luechtefeld T, Coppens I. *Neospora caninum* recruits host cell structures to its parasitophorous vacuole and salvages lipids from organelles. *Eukaryot Cell.* (2015) 14:454–73. doi: 10.1128/EC.00262-14
- Hamid PH, Hirzmann J, Kerner K, Gimpl G, Lochnit G, Hermosilla CR, et al. *Eimeria bovis* infection modulates endothelial host cell cholesterol metabolism for successful replication. *Vet Res.* (2015) 46:100. doi: 10.1186/s13567-015-0230-z
- Simons K, Ikonen E. How cells handle cholesterol. *Science.* (2000) 290:1721–6. doi: 10.1126/science.290.5497.1721
- Ikonen E. Cellular cholesterol trafficking and compartmentalization. *Nat Rev Mol Cell Biol.* (2008) 9:125–38. doi: 10.1038/nrm2336
- Nolan SJ, Romano JD, Coppens I. Host lipid droplets: an important source of lipids salvaged by the intracellular parasite *Toxoplasma gondii*. *PLoS Pathog.* (2017) 13:e1006362. doi: 10.1371/journal.ppat.1006362
- Hu X, Binns D, Reese ML. The coccidian parasites *Toxoplasma* and *Neospora* dysregulate mammalian lipid droplet biogenesis. *J Biol Chem.* (2017) 292:11009–20. doi: 10.1074/jbc.M116.768176
- Petersen W, Stenzel W, Silvie O, Blanz J, Saftig P, Matuschewski K, et al. Sequestration of cholesterol within the host late endocytic pathway restricts liver-stage *Plasmodium* development. *Mol Biol Cell.* (2017) 28:726–35. doi: 10.1091/mbc.E16-07-0531
- Silva LMR, Velásquez ZD, López-Osorio S, Hermosilla C, Taubert A. Novel insights into sterol uptake and intracellular cholesterol trafficking during *Eimeria bovis* macromeront formation. *Front Cell Infect Microbiol.* (2022) 12:809606. doi: 10.3389/fcimb.2022.809606
- Taubert A, Zahner H, Hermosilla C. Dynamics of transcription of immunomodulatory genes in endothelial cells infected with different coccidian parasites. *Vet Parasitol.* (2006) 142:214–22. doi: 10.1016/j.vetpar.2006.07.021
- Cenedella RJ. Cholesterol synthesis inhibitor U18666A and the role of sterol metabolism and trafficking in numerous pathophysiological processes. *Lipids.* (2009) 44:477–87. doi: 10.1007/s11745-009-3305-7
- Schneider CA, Rasband WS, Eliceiri KW. NIH image to ImageJ: 25 years of image analysis. *Nat Methods.* (2012) 9:671–5. doi: 10.1038/nmeth.2089
- Phillips MC. Molecular mechanisms of cellular cholesterol efflux. *J Biol Chem.* (2014) 289:24020–9. doi: 10.1074/jbc.R114.583658
- Maxfield FR, Wüstner D. Analysis of cholesterol trafficking with fluorescent probes. *Methods Cell Biol.* (2012) 108:367–93. doi: 10.1016/B978-0-12-386487-1.00017-1
- Elgner F, Ren H, Medvedev R, Ploen D, Himmelsbach K, Boller K, et al. The intracellular cholesterol transport inhibitor U18666A inhibits the exosome-dependent release of mature hepatitis C virus. *J Virol.* (2016) 90:11181–96. doi: 10.1128/JVI.01053-16
- Poh MK, Shui G, Xie X, Shi PY, Wenk MR, Gu F. U18666A, an intra-cellular cholesterol transport inhibitor, inhibits dengue virus entry and replication. *Antiviral Res.* (2012) 93:191–8. doi: 10.1016/j.antiviral.2011.11.014
- Song B. The cholesterol transport inhibitor U18666A interferes with pseudorabies virus infection. *Viruses.* (2022) 14:1539. doi: 10.3390/v14071539
- Takano T, Endoh M, Fukatsu H, Sakurada H, Doki T, Hohdatsu T. The cholesterol transport inhibitor U18666A inhibits type I feline coronavirus infection. *Antiviral Res.* (2017) 145:96–102. doi: 10.1016/j.antiviral.2017.07.022
- Sandoz PA, Tremblay C, van der Goot FG, Frechin M. Image-based analysis of living mammalian cells using label-free 3D refractive index maps reveals new organelle dynamics and dry mass flux. *PLoS Biol.* (2019) 17:e3000553. doi: 10.1371/journal.pbio.3000553
- Juhl AD, Wüstner D. Pathways and mechanisms of cellular cholesterol efflux—insight from imaging. *Front Cell Dev Biol.* (2022) 10:834408. doi: 10.3389/fcell.2022.834408
- Horcajo P, Xia D, Randle N, Collantes-Fernández E, Wastling J, Ortega-Mora LM, et al. Integrative transcriptome and proteome analyses define marked differences between *Neospora caninum* isolates throughout the tachyzoite lytic cycle. *J Proteome.* (2018) 180:108–19. doi: 10.1016/j.jpro.2017.11.007
- Taubert A, Wimmers K, Ponsuksili S, Jimenez CA, Zahner H, Hermosilla C. Microarray-based transcriptional profiling of *Eimeria bovis*-infected bovine endothelial host cells. *Vet Res.* (2010) 41:70. doi: 10.1051/vetres/2010041
- Jelinek D, Castillo JJ, Richardson LM, Luo L, Heidenreich RA, Garver WS. The Niemann–Pick C1 gene is downregulated in livers of C57BL/6J mice by dietary fatty acids, but not dietary cholesterol, through feedback inhibition of the SREBP pathway. *J Nutr.* (2012) 142:1935–42. doi: 10.3945/jn.112.162818
- Gévry N, Schoonjans K, Guay F, Murphy BD. Cholesterol supply and SREBPs modulate transcription of the Niemann–Pick C-1 gene in steroidogenic tissues. *J Lipid Res.* (2008) 49:1024–33. doi: 10.1194/jlr.M700554-JLR200
- Millard EE, Srivastava K, Traub LM, Schaffer JE, Ory DS. Niemann–Pick type C1 (NPC1) overexpression alters cellular cholesterol homeostasis. *J Biol Chem.* (2000) 275:38445–51. doi: 10.1074/jbc.M003180200
- Horcajo P, Jiménez-Pelayo L, García-Sánchez M, Regidor-Cerrillo J, Collantes-Fernández E, Rozas D, et al. Transcriptome modulation of bovine trophoblast cells *in vitro* by *Neospora caninum*. *Int J Parasitol.* (2017) 47:791–9. doi: 10.1016/j.ijpara.2017.08.007